Vol 18 No 2, February 2009
1674-1056/2009/18(02)/0571-10

Chinese Physics B

© 2009 Chin. Phys. Soc.
and IOP Publishing Ltd

Propagation of the off-axis superposition of partially coherent beams through atmospheric turbulence*

Zhang En-Tao(张恩涛)[a)b)], Ji Xiao-Ling(季小玲)[c)], and Lü Bai-Da(吕百达)[a)†]

[a)] *Institute of Laser Physics and Chemistry, Sichuan University, Chengdu* 610064, *China*
[b)] *School of Sciences of Southwest Petroleum University, Chengdu* 610500, *China*
[c)] *College of Electronic Engineering, Sichuan Normal University, Chengdu* 610066, *China*

(Received 14 November 2007; revised manuscript received 30 June 2008)

The propagation properties of the off-axis superposition of partially coherent beams through atmospheric turbulence and their beam quality in terms of the mean-squared beam width $w(z)$ and the power in the bucket (PIB) are studied in detail, where the effects of partial coherence, off-axis beam superposition and atmospheric turbulence are considered. The analytical expressions for the intensity, the beam width and the PIB are derived, and illustrative examples are given numerically. It is shown that the maximum intensity $I_{\max}$ and the PIB decrease and $w(z)$ increases as the refraction index structure constant $C_{\rm n}^2$ increases. Therefore, the turbulence results in a degradation of the beam quality. However, the resulting partially coherent beam with a smaller value of spatial correlation parameter γ and larger values of separate distance $x_{\rm d}$ and beam number M is less affected by the turbulence than that with a larger value of γ and smaller values of $x_{\rm d}$ and M. The main results obtained in this paper are explained physically.

Keywords: off-axis superposition of partially coherent beams, atmospheric turbulence, propagation property, beam quality

PACC: 4225B, 4225K, 9265R

1. Introduction

The off-axis superposition of beams is a subject of current interest for scaling diode arrays, CO_2 and HF/DF chemical lasers, etc. up to high-power level.[1,2] The coherent beam superposition and the incoherent beam superposition with linear, rectangular and radial array geometries for coherent off-axis Gaussian beams, Hermite–Gaussian beams, etc., have been studied.[2−5] In practice, a partially coherent laser source is often encountered. Recently, the characteristics of the off-axis superposition of partially coherent beams were studied theoretically and numerically by using the Wigner distribution function.[6] On the other hand, the propagation properties of laser beams through atmospheric turbulence are of importance for many practical applications such as the remote sensing, atmospheric optical communication, etc.[7,8] It was demonstrated both theoretically and experimentally that partially coherent beams were less sensitive to the effect of turbulence than fully coherent ones.[9−14] Very recently, the propagation of $M \times N$ Gaussian beams through turbulent atmosphere and their beam quality were investigated in Ref.[15].

In the present paper, the Gaussian–Schell model (GSM) beam is taken as an example of the partially coherent beam. The propagation properties of the off-axis superposition of partially coherent beams through atmospheric turbulence and their beam quality in terms of the mean-squared beam width and the power in the bucket (PIB)[16] are studied theoretically and numerically. Some interesting results are obtained and explained physically.

2. Propagation equation of the off-axis superposition of partially coherent beams

The cross-spectral density function of a two-dimensional GSM beam in the plane $z = 0$ is given by

*Project supported by the National Natural Science Foundation of China (Grant No 60778048).
†Corresponding author. E-mail: Baidalu0@tom.com; Entaozhang@163.com

$$
\begin{aligned}
&W_1^{(0)}(x_1', x_2', z=0)\\
&= \langle E(x_1')E^*(x_2')\rangle\\
&= \exp\left(-\frac{x_1'^2+x_2'^2}{w_0^2}\right)\exp\left(-\frac{(x_1'-x_2')^2}{2\sigma_0^2}\right), \quad (1)
\end{aligned}
$$

where the point brackets denote an ensemble average, the asterisk represents the complex conjugate; w_0 and σ_0 are waist width and correlation length of the GSM beam, respectively. It is worth mentioning that to clarify the main physical results, the mathematical manipulation is performed in the two-dimensional case within the framework of the paraxial approximation, but the extension to the three-dimensional case is straightforward, because the variables x and y are separable.

Now we assume that M individual off-axis GSM beamlets are positioned along the x-axis in the plane $z=0$ whose separate distance is x_d, For definiteness let M be an odd number. The cross-spectral density function of the resulting partially coherent beam in the plane $z=0$ is expressed as

$$
\begin{aligned}
&W^0(x_1', x_2', z=0)\\
&= \left\langle \left(\sum_m E(x_1'-mx_\mathrm{d})\right)\left(\sum_n E(x_2'-nx_\mathrm{d})\right)^* \right\rangle\\
&= \sum_{m=-\frac{M-1}{2}}^{\frac{M-1}{2}} \sum_{n=-\frac{M-1}{2}}^{\frac{M-1}{2}} \left\{ \exp\left[-\frac{(x_1'-mx_\mathrm{d})^2+(x_2'-nx_\mathrm{d})^2}{w_0^2}\right] \times \exp\left[-\frac{[(x_1'-mx_\mathrm{d})-(x_2'-nx_\mathrm{d})]^2}{2\sigma_0^2}\right]\right\}. \quad (2)
\end{aligned}
$$

By using the extended Huygens–Fresnel principle, the cross-spectral density function of the resulting partially coherent beam represented by expression (2), propagating through atmospheric turbulence, reads as follows:[8]

$$
\begin{aligned}
W(x_1,x_2,z) = \frac{k}{2\pi z}\int_{-\infty}^{\infty}\int_{-\infty}^{\infty} \mathrm{d}x_1'\mathrm{d}x_2' W^{(0)}(x_1', x_2', z=0)\exp\left\{\frac{\mathrm{i}k}{2z}\left[(x_1'^2-x_2'^2)-2(x_1x_1'-x_2x_2')+(x_1^2-x_2^2)\right]\right\}\\
\times\langle\exp[\psi(x_1',x_1)+\psi^*(x_2',x_2)]\rangle_m, \quad (3)
\end{aligned}
$$

where k is the wave number related to the wave length λ by $k=2\pi/\lambda$, $\psi(x',x)$ represents the random part of the complex phase of a spherical wave due to the turbulence. $\langle\,\rangle_m$ denotes the average over the ensemble of the turbulent medium statistics, and[17,18]

$$
\langle\exp\left[\psi(x_1',x_1)+\psi^*(x_2',x_2)\right]\rangle_m \cong \exp\left[-\frac{(x_1'-x_2')^2+(x_1'-x_2')(x_1-x_2)+(x_1-x_2)^2}{\rho_0^2}\right], \quad (4)
$$

where $\rho_0=\left(0.545C_\mathrm{n}^2k^2z\right)^{-3/5}$ is the coherence length in turbulence, C_n^2 is the refraction index structure constant, which describes how strong the turbulence is. It is noted that a quadratic approximation of Rytov's phase structure function has been used in expression (3) to obtain an analytical result. This approximation has been shown to be a good approximation for practical situations.[19]

Substituting expressions (2) and (4) into expression (3), letting $x_1=x_2=x$, and recalling the formula yield

$$
\int_{-\infty}^{\infty}\exp(-p^2t^2+qt)\mathrm{d}t = \frac{\sqrt{\pi}}{p}\exp\left(\frac{q^2}{4p^2}\right). \quad (5)
$$

And after very tedious but straightforward integral calculations, we obtain the closed-form propagation equation of the resulting partially coherent beam through atmospheric turbulence, which is given by

$$
\begin{aligned}
I(x,z)=W(x,x,z) = \frac{k}{2zH}\sum_{m=-\frac{M-1}{2}}^{\frac{M-1}{2}}\sum_{n=-\frac{M-1}{2}}^{\frac{M-1}{2}}\exp\left[-\left(\frac{k^2A^2S^2}{4z^2H^2}+\frac{k^2}{4A^2z^2}\right)x^2+\left(\frac{\mathrm{i}kA^2RS}{2zH^2}-\frac{\mathrm{i}kT}{2zA^2}\right)x\right.\\
\left.+\frac{mnx_\mathrm{d}^2}{\sigma_0^2}-\left(\frac{1}{w_0^2}+\frac{1}{2\sigma_0^2}\right)(m^2+n^2)x_\mathrm{d}^2+\frac{A^2R^2}{4H^2}+\frac{T^2}{4A^2}\right], \quad (6)
\end{aligned}
$$

where

$$A = \sqrt{\frac{1}{w_0^2} + \frac{1}{2\sigma_0^2} + \frac{1}{\rho_0^2} - \frac{\mathrm{i}k}{2z}}, \tag{7}$$

$$R = \frac{2nx_\mathrm{d}}{w_0^2} + \frac{(n-m)x_\mathrm{d}}{\sigma_0^2} + \left(\frac{1}{A^2\rho_0^2} + \frac{1}{2A^2\sigma_0^2}\right)\left(\frac{2mx_\mathrm{d}}{w_0^2} - \frac{(n-m)x_\mathrm{d}}{\sigma_0^2}\right), \tag{8}$$

$$S = 1 - \frac{1}{A^2\rho_0^2} - \frac{1}{2A^2\sigma_0^2}, \tag{9}$$

$$T = \frac{2mx_\mathrm{d}}{w_0^2} + \frac{(m-n)x_\mathrm{d}}{\sigma_0^2}, \tag{10}$$

and

$$H = \sqrt{\frac{1}{w_0^4} + \frac{2}{w_0^2\rho_0^2} + \frac{1}{w_0^2\sigma_0^2} + \frac{k^2}{4z^2}}. \tag{11}$$

From expression (6) together with expressions (7)–(11) it follows that the intensity distribution of the resulting partially coherent beam depends on the partial coherence, off-axis beam superposition, atmospheric turbulence, and propagation distance, i.e. on the beam correlation length σ_0, beam number M, separate distance x_d, refraction index structure constant C_n^2 and propagation distance z.

For $C_\mathrm{n}^2 = 0$, expression (6) reduces to the propagation expression of the resulting partially coherent beam in free space, i.e.

$$I(x,z) = \frac{k\sigma_0 w_0}{\sqrt{g_\mathrm{f}}} \sum_{m=-\frac{M-1}{2}}^{\frac{M-1}{2}} \sum_{n=-\frac{M-1}{2}}^{\frac{M-1}{2}} \exp\left\{\frac{2\sigma_0^2}{g_\mathrm{f} w_0^2}k^2 w_0^2 x^2 + \frac{2kxx_\mathrm{d}}{g_\mathrm{f}}\left\{\mathrm{i}2z(m-n) + \frac{\sigma_0^2}{w_0^2}[\mathrm{i}2z(m-n) + k(m+n)w_0^2]\right\}\right.$$
$$\left. + \frac{2kx_\mathrm{d}^2}{2g_\mathrm{f}}\left\{(m-n)[\mathrm{i}4z(m+n) + k(m-n)w_0^2] + 2\frac{\sigma_0^2}{w_0^2}[\mathrm{i}2z(m^2-n^2) + k(m^2+n^2)w_0^2]\right\}\right\}, \tag{12}$$

where

$$g_\mathrm{f} = 4z^2 + \frac{\sigma_0^2}{w_0^2}(4z^2 + k^2 w_0^4). \tag{13}$$

Expression (12) is in agreement with Eq.(29) in Ref.[6].

For $M = 1$, expression (6) reduces to the propagation expression of a GSM beam through atmospheric turbulence, i.e.

$$I(x,z) = \frac{k}{2zH}\exp\left\{-\frac{k^2x^2}{2z^2A^2H^2}\left[\frac{1}{w_0^4} + \frac{1}{w_0^2}\left(\frac{1}{2\sigma_0^2} + \frac{1}{\rho_0^2} - \frac{\mathrm{i}k}{2z}\right)\right]\right\}, \tag{14}$$

Numerical calculations are performed to illustrate the propagation properties of the resulting partially coherent beam through atmospheric turbulence. Typical examples are given in Figs.1–3, where $\lambda = 1.06 \times 10^{-6}$ m is kept fixed, and the spatial correlation parameter $\gamma = [1 + (w_0/\sigma_0)^2]^{-1/2}$ is used. The smaller the value of γ is, the worse the beam spatial coherence will be, and $\gamma = 1$ corresponds to the fully coherent beam. The distributions of relative intensity $I(x,z)/I_\mathrm{max}$ of resulting partially coherent beams versus propagation distance z and refraction index structure constant C_n^2 are plotted in Figs.1(a) and 1(b) respectively. Figure 1(a) indicates that the resulting partially coherent beam propagating through atmospheric turbulence undergoes three stages of evolution with propagation distance z increasing, i.e. its beam profile is similar to the initial one at $z = 2.5$ km, and then it becomes a flat-top profile with z increasing ($z = 4$ km), finally it turns into Gaussian-like profile in the far field ($z = 10$ km). In addition, Fig.1(b) shows that the turbulence speeds up the evolution of the three stages, which the resulting partially coherent beam undergoes. The results of the off-axis superstition of partially coherent beams in Figs.1(a) and 1(b) are similar to those of a fully or partially coherent beam propagating through atmospheric turbulence.[18,20]

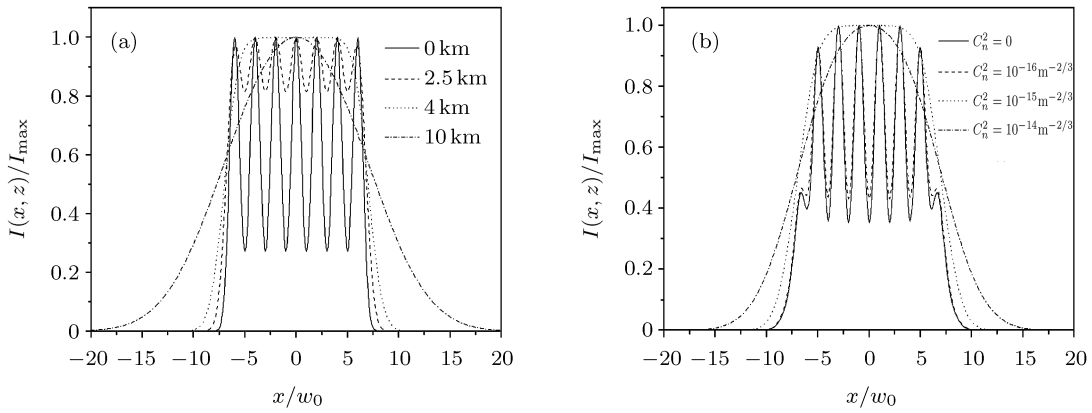


Fig.1. The distributions of relative intensity $I(x,z)/I_{\max}$ of resulting partially coherent beams (a) for different values of z, with the calculation parameters being $w_0 = 0.05\,\mathrm{m}$, $x_\mathrm{d}/w_0 = 3$, $M = 7$, $\gamma = 0.5$ and $C_\mathrm{n}^2 = 2\times10^{-15}\,\mathrm{m}^{-2/3}$; (b) for different values of C_n^2, with the calculation parameters being $w_0 = 0.05\,\mathrm{m}$, $x_\mathrm{d}/w_0 = 2$, $M = 7$, $\gamma = 0.5$ and $z = 8\,\mathrm{km}$.

The distributions of relative intensity $I(x,z)/I_{\max}$ of resulting partially coherent beams with different values of the relative separate distance x_d/w_0 and the spatial correlation parameter γ are shown in Figs.2(a) and 2(b) respectively. From Fig.2(a) we see that with x_d/w_0 decreasing, the resulting partially coherent beam propagating through atmospheric turbulence undergoes three stages of evolution at a certain propagation distance, e.g. $z = 8\,\mathrm{km}$, its beam profile is similar to the initial one for $x_\mathrm{d}/w_0 = 4$, and then it becomes a flat-top profile for $x_\mathrm{d}/w_0 = 2$, finally it turns into Gaussian-like profile for $x_\mathrm{d}/w_0 = 1$. Figure 2(b) indicates that the intensity distribution in the plane $z = 16\,\mathrm{km}$ becomes smooth and narrow with γ increasing, and for $\gamma = 0.9$ its beam profile turns into Gaussian-like one.

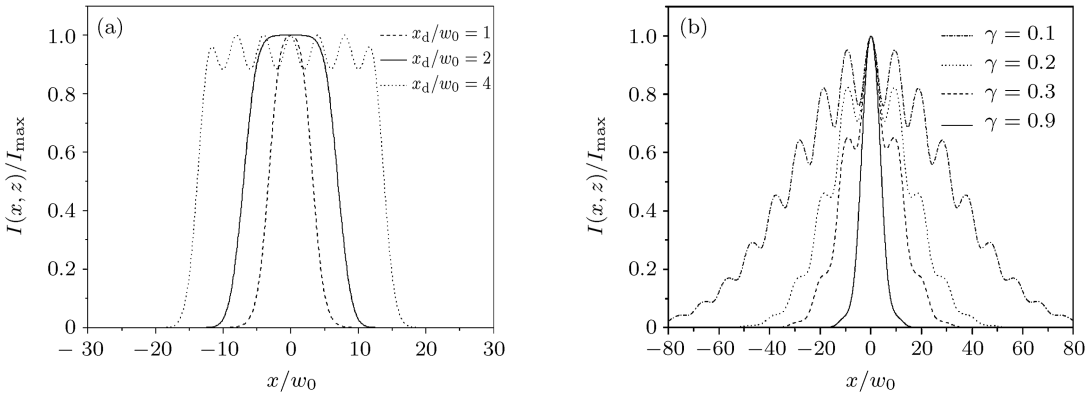


Fig.2. The distributions of relative intensity $I(x,z)/I_{\max}$ of resulting partially coherent beams (a) for different values of x_d/w_0, with the calculation parameters being $w_0 = 0.05\,\mathrm{m}$, $M = 7$, $\gamma = 0.5$, $C_\mathrm{n}^2 = 2\times10^{-15}\,\mathrm{m}^{-2/3}$ and $z = 8\,\mathrm{km}$; (b) for different values of γ, with the calculation parameters being $w_0 = 0.03\,\mathrm{m}$, $x_\mathrm{d}/w_0 = 2$, $M = 7$, $C_\mathrm{n}^2 = 3\times10^{-15}\,\mathrm{m}^{-2/3}$ and $z = 16\,\mathrm{km}$.

The distributions of relative intensity $I(x,z)/I_{0\,\max}$ of resulting partially coherent beams are given in Figs.3(a)–3(d) for different values of γ, where $I_{0\,\max}$ is the maximum intensity of the corresponding resulting partially coherent beam in free space. From Fig.3 we can see that the larger the value of γ is, the smaller the maximum intensity $I_{\max}$ in turbulence will be as compared with the scenario in free space. For example, for $\gamma = 0.2$, 0.4, 0.6 and 0.9, we have $I_{\max}/I_{0\,\max} = 0.51$, 0.42, 0.38 and 0.36 respectively. Thus, the maximum intensity of the resulting partially coherent beam with a smaller value of γ is less affected by the turbulence than that with a larger value of γ.

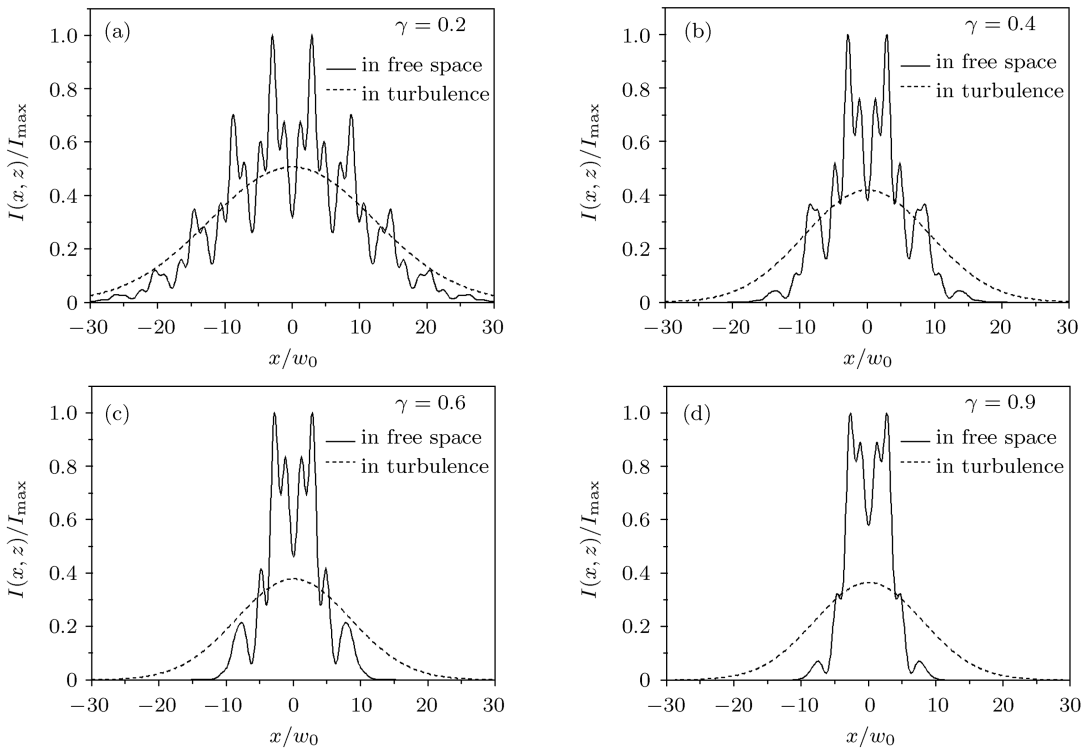


Fig.3. The distributions of relative intensity $I(x,z)/I_{0\,\max}$ of resulting partially coherent beams in free space and in turbulence ($C_{\rm n}^2 = 10^{-14}\,{\rm m}^{-2/3}$) for different values of γ, with the calculation parameters being $w_0 = 0.03\,{\rm m}$, $x_{\rm d}/w_0 = 2$, $M = 5$ and $z = 10\,{\rm km}$.

3. Mean-squared beam width

The mean-squared beam width is defined as[3,16]

$$w^2(z) = \frac{\int_{-\infty}^{\infty} x^2 I(x,z)\mathrm{d}x}{\int_{-\infty}^{\infty} I(x,z)\mathrm{d}x}. \tag{15}$$

Substituting expression (6) into expression (15), after very tedious integral calculations (see Appendix A) we obtain

$$w^2(z) = \sum_{m=-\frac{M-1}{2}}^{\frac{M-1}{2}} \sum_{n=-\frac{M-1}{2}}^{\frac{M-1}{2}} \left(\frac{1}{2Q} + \frac{P^2}{4Q^2}\right) U \Bigg/ \sum_{m=-\frac{M-1}{2}}^{\frac{M-1}{2}} \sum_{n=-\frac{M-1}{2}}^{\frac{M-1}{2}} U, \tag{16}$$

where

$$U = \exp\left[\frac{mnx_{\rm d}^2}{\sigma_0^2} - \left(\frac{1}{w_0^2} + \frac{1}{2\sigma_0^2}\right)(m^2+n^2)x_{\rm d}^2 + \frac{A^2R^2}{4H^2} + \frac{T^2}{4A^2} + \frac{P^2}{4Q}\right], \tag{17}$$

$$P = \frac{\mathrm{i}kA^2RS}{2zH^2} - \frac{\mathrm{i}kT}{2zA^2}, \tag{18}$$

and

$$Q = \frac{k^2A^2S^2}{4z^2H^2} + \frac{k^2}{4A^2z^2}. \tag{19}$$

From expression (16) together with expressions (17)–(19) it follows that the mean squared beam width of the resulting beam depends on $\sigma_0(\gamma)$, M, $x_{\rm d}$, $C_{\rm n}^2$ and z.

The curves for relative width $w(z)/w(0)$ of resulting partially coherent beams propagating through atmospheric turbulence versus propagation distance z for different values of γ, $x_{\rm d}/w_0$ and M are given in Figs.4(a), 4(b) and 4(c) respectively. Figure 4(a) shows that the beam spreading in free space is smaller than that in atmospheric turbulence for different val-

ues of γ. However, the relative difference in beam width of the resulting partially coherent beam between in turbulence and in free space, $\Delta w/w(0) = w(z)/w(0)|_{\rm turb} - w(z)/w(0)|_{\rm free}$, increases as γ increases. For example, for $\gamma = 0.2$, 0.3, and 0.9, we have $\Delta w/w(0) = 0.6$, 0.76 and 1.09 in the plane $z = 10$ km, respectively. Thus, the relative spreading of the resulting partially coherent beam with a smaller value of γ is less affected by the turbulence than that of the resulting partially coherent beam with a larger value of γ. From Fig.4(b) it can be seen that $\Delta w/w(0)$ decreases as $x_{\rm d}/w_0$ increases, e.g. for $x_{\rm d}/w_0 = 2$, 3, and 4, we have $\Delta w = 0.93$, 0.53 and 0.34 in the plane $z = 10$ km, respectively. Figure 4(c) shows that Δw decreases with M increasing, e.g. for $M = 3$, 5, and 7, we have $\Delta w = 1.87$, 0.86 and 0.53 in the plane $z = 10$ km, respectively.

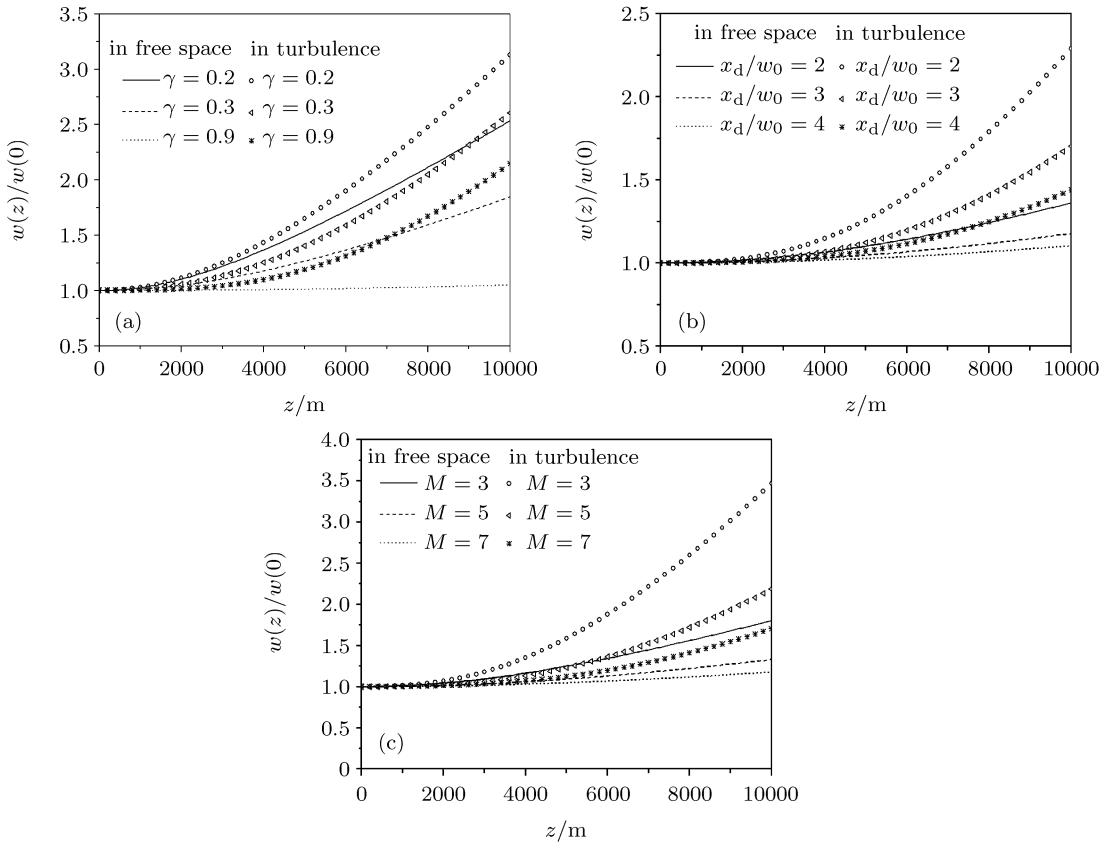


Fig.4. The curves for relative width $w(z)/w(0)$ of resulting partially coherent beams with $w_0 = 0.03$ m in free space and in turbulence ($C_{\rm n}^2 = 10^{-14}\,{\rm m}^{-2/3}$) (a) for different values of γ, with the calculation parameters being $M = 7$ and $x_{\rm d}/w_0 = 2$; (b) for different values of $x_{\rm d}/w_0$, with the calculation parameters being $M = 7$ and $\gamma = 0.5$; (c) for different values of M, with the calculation parameters being $\gamma = 0.5$ and $x_{\rm d}/w_0 = 3$.

4. Power in the bucket (PIB)

The beam propagation factor (M^2-factor) and PIB are the parameters for characterizing beam quality.[16] The PIB is a useful method of characterizing different laser beams, and it is essentially a measure of laser power focusability in the far field, which is defined as the fractional power within a given bucket size in the far field. The larger the value of PIB is, the better the laser power focusability will be, and the better the beam quality will be. For practical applications of laser beams propagating through atmospheric turbulence we are often interested in the beam power (energy) focusability in the far field, but the smaller value of M^2-factor does not necessarily correspond to the better focusability for the off-axis beam superposition.[5] Therefore, in this paper the PIB is chosen as a characteristic parameter of the beam quality in the far field, which is given by[16]

$$\mathrm{PIB} = \frac{\int_{-b}^{b} I(x,z)\mathrm{d}x}{\int_{-\infty}^{\infty} I(x,z)\mathrm{d}x}, \tag{20}$$

where b is the bucket half width chosen.

Substituting expression (6) into expression (20), after very tedious integral calculations (see Appendix B) we obtain

$$\mathrm{PIB} = \sum_{m=-\frac{M-1}{2}}^{\frac{M-1}{2}} \sum_{n=-\frac{M-1}{2}}^{\frac{M-1}{2}} \left[\mathrm{erf}\left(\frac{P+2bQ}{2\sqrt{Q}}\right) - \mathrm{erf}\left(\frac{P-2bQ}{2\sqrt{Q}}\right)\right] U \Big/ 2 \sum_{m=-\frac{M-1}{2}}^{\frac{M-1}{2}} \sum_{n=-\frac{M-1}{2}}^{\frac{M-1}{2}} U, \tag{21}$$

where erf is the error function. From expression (21) it is easy to see that the PIB in the z plane in the far field is dependent on $\sigma_0(\gamma)$, M, x_d and C_n^2.

The PIB curves of resulting partially coherent beams in atmospheric turbulence in the plane $z = 8\,\mathrm{km}$ are depicted in Figs.5(a)–5(c). Figure 5(a) shows that the values of PIB in turbulence and in free space decrease with γ decreasing. However, the difference in PIB of the resulting partially coherent beam between in turbulence and in free space, $\Delta\mathrm{PIB} = \mathrm{PIB}|_\mathrm{turb} - \mathrm{PIB}|_\mathrm{free}$, increases as γ increases. For example, for PIB = 63%, γ = 0.2, 0.4 and 0.9, we have ΔPIB = 1.38, 2.14 and 2.55, respectively. From Fig.5(b) it can be seen that ΔPIB decreases with x_d/w_0 increasing, e.g. for PIB = 63%, x_d/w_0 = 1, 2 and 3, we have ΔPIB = 3.64, 2.33 and 1.86, respectively. Figure 5(c) shows that ΔPIB decreases with M increasing, e.g. for PIB = 63%, M = 3, 5 and 7, we have ΔPIB = 2.77, 2.23 and 1.87, respectively. Therefore, the relative spreading of the resulting partially coherent beam with a smaller value of γ and larger values of x_d and M is less affected by the turbulence than that of the resulting partially coherent beam with a larger value of γ and smaller values of x_d and M.

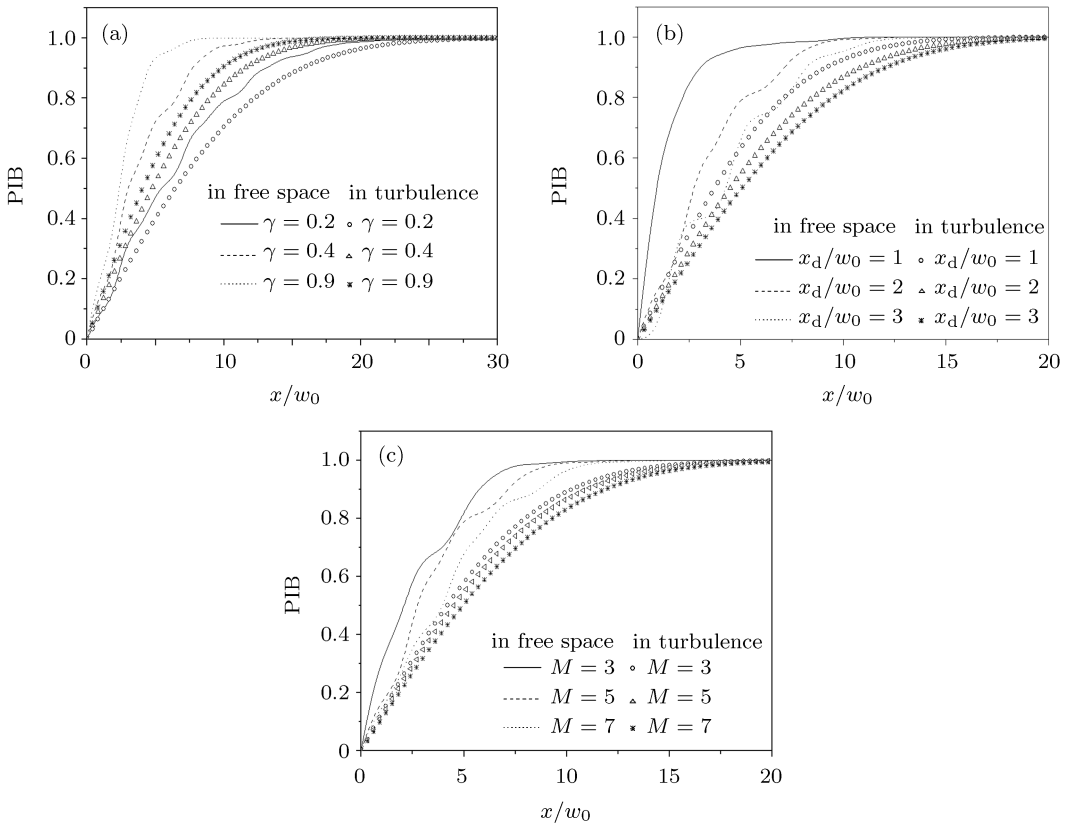


Fig.5. PIB curves of resulting partially coherent beams with $w_0 = 0.03\,\mathrm{m}$ in free space and in turbulence ($C_\mathrm{n}^2 = 10^{-14}\,\mathrm{m}^{-2/3}$) in the plane $z = 8\,\mathrm{km}$ (a) for different values of γ, with the calculation parameters being $M = 5$ and $x_\mathrm{d}/w_0 = 2$; (b) for different values of x_d/w_0, with the calculation parameters being $M = 7$ and $\gamma = 0.5$; (c) for different values of M, with the calculation parameters being $\gamma = 0.5$ and $x_\mathrm{d}/w_0 = 2$.

5. Physical explanations

The curves for mean-squared beam width $w(z)$ of the resulting partially coherent beam in free space ($C_{\rm n}^2 = 0$) versus propagation distance z for different values of γ, $x_{\rm d}/w_0$ and M are shown in Figs.6(a)–6(c), respectively. Figure 6(a) shows that in the plane $z = 0$, $w(0)$ is nearly unchanged for different values of γ. But, as the propagation distance z increases, $w(z)$ increases apparently with γ decreasing in free space. From Figs.6(b) and 6(c) it follows that $w(z)$ increases with $x_{\rm d}/w_0$ and M increasing in free space.

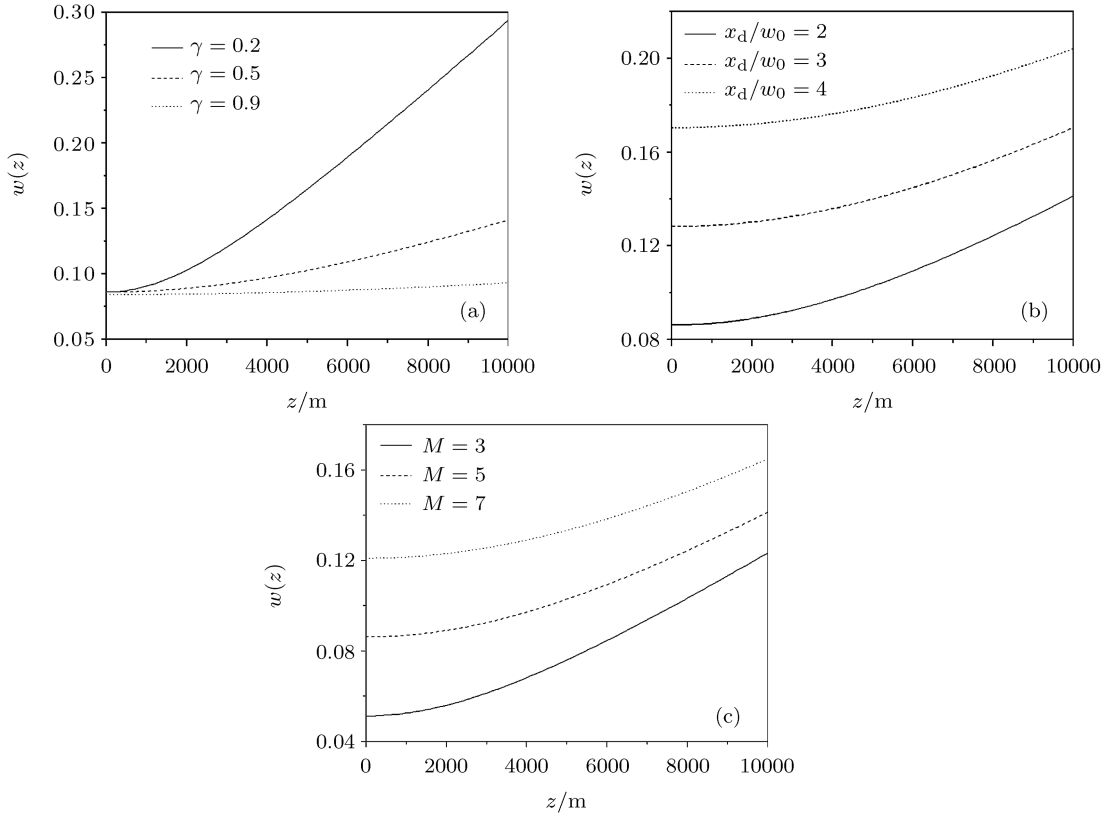


Fig.6. The curves for mean-squared beam width $w(z)$ of resulting partially coherent beams with $w_0 = 0.03$ m in free space (a) for different values of γ, with the calculation parameters being $M = 5$ and $x_{\rm d}/w_0 = 2$; (b) for different values of $x_{\rm d}/w_0$, with the calculation parameters being $M = 5$ and $\gamma = 0.5$; (c) for different values of M, with the calculation parameters being $\gamma = 0.5$ and $x_{\rm d}/w_0 = 2$.

Generally speaking, the spreading of the resulting partially coherent beam propagating through atmospheric turbulence is affected through two mechanisms. One is the free-space diffraction, and the other is the atmospheric turbulence.[10,21] In free space the spreading of the resulting partially coherent beam is due to the free-space diffraction that is related to the beam width w_0, spatial correlation parameter γ and superimposed beam parameters $x_{\rm d}$ and M. Physically, the existence of any additional beam spreading (e.g. partial coherence,[10] higher-order mode operation,[22] etc.) reduces the influence of atmospheric turbulence. From Fig.6 we see that the smaller the value of γ is and the larger the values of $x_{\rm d}$ and M are, the more rapidly the resulting partially coherent beam spreads in free space. This is the physical reason why the relative spreading of the resulting partially coherent beam with a smaller value of spatial coherent parameter γ and larger values of separate distribution $x_{\rm d}$ and beam number M is less affected by the turbulence than that with a larger value of γ and smaller values of $x_{\rm d}$ and M.

6. Conclusions

Based on the extended Huygens–Fresnel principle, the propagation of the off-axis superposition of partially coherent beams through atmospheric turbulence and their beam quality have been studied. The closed-form expressions for the intensity, the beam

width and the PIB are derived. It is shown both theoretically and numerically that the intensity distribution, the mean-squared beam width and the PIB of the resulting partially coherent beam depend on refraction index structure constant C_{n}^2, spatial correlation parameter γ, separate distance x_{d}, beam number M and propagation distance z. The intensity distribution becomes smooth and narrow with spatial correlation parameter γ increasing and even turns into Gaussian-like profile when γ is large enough. The maximum intensity $I_{\max}$ and the PIB decrease and $w(z)$ increases with C_{n}^2 increasing. Therefore, the turbulence results in a degradation of the beam quality. However, $I_{\max}$ of the resulting partially coherent beam with a smaller value of γ is less affected by the turbulence than that of the resulting partially coherent beam with a larger value of γ. The relative spreading of the resulting partially coherent beam with a smaller value of γ and larger values of x_{d} and M is less affected by the turbulence than that with a larger value of γ and smaller values of x_{d} and M. The results obtained in this paper would be useful for studying superimposed partially coherent laser beams passing through atmospheric turbulence.

Appendix A: Derivation of expression (16)

Expression (15) can be rewritten as

$$w^2(z) = \frac{\delta}{\eta}, \tag{A1}$$

where

$$\eta = \int_{-\infty}^{\infty} I(x,z)\mathrm{d}x, \tag{A2}$$

and

$$\delta = \int_{-\infty}^{\infty} x^2 I(x,z)\mathrm{d}x. \tag{A3}$$

Recalling the formula (5) and substituting expression (6) into expression (A2) lead to

$$\eta = \frac{k\sqrt{\pi}}{2\pi H\sqrt{Q}} \sum_{m=-\frac{M-1}{2}}^{\frac{M-1}{2}} \sum_{n=-\frac{M-1}{2}}^{\frac{M-1}{2}} \exp\left[\frac{mnx_{\mathrm{d}}^2}{\sigma_0^2} - \left(\frac{1}{w_0^2}+\frac{1}{2\sigma_0^2}\right)(m^2+n^2)x_{\mathrm{d}}^2 + \frac{A^2R^2}{4H^2} + \frac{T^2}{4A^2} + \frac{P^2}{4Q}\right]. \tag{A4}$$

Substituting expression (6) into expression (A3), and recalling the formula

$$\int_{-\infty}^{\infty} t^2 \exp(-\mu t^2 + 2vt)\mathrm{d}t = \frac{1}{2\mu}\sqrt{\frac{\pi}{\mu}}\left(1+2\frac{v^2}{\mu}\right)\exp\left(\frac{v^2}{\mu}\right), \tag{A5}$$

we obtain

$$\delta = \frac{k}{2\pi H} \sum_{m=-\frac{M-1}{2}}^{\frac{M-1}{2}} \sum_{n=-\frac{M-1}{2}}^{\frac{M-1}{2}} \exp\left[\frac{mnx_{\mathrm{d}}^2}{\sigma_0^2} - \left(\frac{1}{w_0^2}+\frac{1}{2\sigma_0^2}\right)(m^2+n^2)x_{\mathrm{d}}^2 + \frac{A^2R^2}{4H^2} + \frac{T^2}{4A^2} + \frac{P^2}{4Q}\right] \frac{\sqrt{\pi}}{2\sqrt{Q^3}}\left(1+\frac{P^2}{4Q}\right). \tag{A6}$$

Substituting expressions (A4) and (A6) into expression (A1) yields

$$w^2(z) = \sum_{m=-\frac{M-1}{2}}^{\frac{M-1}{2}} \sum_{n=-\frac{M-1}{2}}^{\frac{M-1}{2}} \left(\frac{1}{2Q}+\frac{P^2}{4Q^2}\right) U \Bigg/ \sum_{m=-\frac{M-1}{2}}^{\frac{M-1}{2}} \sum_{n=-\frac{M-1}{2}}^{\frac{M-1}{2}} U. \tag{A7}$$

Appendix B: Derivation of expression (21)

Expression (20) can be rewritten as

$$\mathrm{PIB} = \frac{\tau}{\eta}, \tag{B1}$$

where

$$\tau = \int_{-b}^{b} I(x,z)\mathrm{d}x, \tag{B2}$$

and η is defined in the form of expression (A2).

Substituting expression (6) into expression (B2) and recalling the formula

$$\mathrm{erf}(b) = \int_{-b}^{b} \exp(-t^2)\mathrm{d}t, \tag{B3}$$

the integral calculations lead to

$$\tau = \frac{k\sqrt{\pi}}{4\pi H\sqrt{Q}} \sum_{m=-\frac{M-1}{2}}^{\frac{M-1}{2}} \sum_{n=-\frac{M-1}{2}}^{\frac{M-1}{2}} \exp\left[\frac{mnx_{\mathrm{d}}^2}{\sigma_0^2} - \left(\frac{1}{w_0^2} + \frac{1}{2\sigma_0^2}\right)(m^2+n^2)x_{\mathrm{d}}^2 + \frac{A^2R^2}{4H^2} + \frac{T^2}{4A^2} + \frac{P^2}{4Q}\right]$$

$$\times \left[\mathrm{erf}\left(\frac{P+2bQ}{2\sqrt{Q}}\right) - \mathrm{erf}\left(\frac{P-2bQ}{2\sqrt{Q}}\right)\right]. \tag{B4}$$

Substituting expressions (A4) and (B4) into expression (B1) yields

$$\mathrm{PIB} = \sum_{m=-\frac{M-1}{2}}^{\frac{M-1}{2}} \sum_{n=-\frac{M-1}{2}}^{\frac{M-1}{2}} \left[\mathrm{erf}\left(\frac{P+2bQ}{2\sqrt{Q}}\right) - \mathrm{erf}\left(\frac{P-2bQ}{2\sqrt{Q}}\right)\right] U \Big/ 2 \sum_{m=-\frac{M-1}{2}}^{\frac{M-1}{2}} \sum_{n=-\frac{M-1}{2}}^{\frac{M-1}{2}} U. \tag{B5}$$

References

[1] Strohschein J D, Herb J J and Clarence E C 1998 *Appl. Opt.* **37** 1045

[2] Brunel M, Floch A L, Bretenaker F, Marty J and Molva E 1998 *Appl. Opt.* **37** 2402

[3] Chodzko R A, Bernard J M and Mirels H 1990 *Proc. SPIE* **1224** 239

[4] Andrews J R 1989 *Opt. Lett.* **14** 33

[5] Lü B D and Ma H 2000 *Appl. Opt.* **39** 1279

[6] Li B Z and Lü B D 2003 *J. Opt.* A: *Pure and Appl. Opt.* **5** 303

[7] Fante R L 1985 *Progress in Optics* XXII ed Wolf E (Amsterdam: Elsevier) Chapter VI

[8] Andrews L C and Phillips R L 1998 *Laser Beam Propagation Through Random Media* (Bellingham, WA: SPIE Press)

[9] Wu J 1990 *J. Mod. Opt.* **37** 671

[10] Gbur G and Wolf E 2002 *J. Opt. Soc. Am.* A **19** 1592

[11] Dogariu A and Amarande S 2003 *Opt. Lett.* **28** 10

[12] Ji X L and Lü B D 2005 *Opt. Commun.* **251** 231

[13] Ji X L, Huang T X and Lü B D Y 2006 *Acta Phys. Sin.* **55** 978 (in Chinese)

[14] Ji X L, Lü B D and Xiao X 2004 *Acta Phys. Sin.* **53** 3996 (in Chinese)

[15] Ji X L, Zhang E T and Lü B D 2006 *J. Mod. Opt.* **53** 2111

[16] Siegman A E 1998 *OSA. TOPS* **17** 184

[17] Yura H T 1972 *Appl. Opt.* **11** 1399

[18] Eyyuboglu H T 2005 *Opt. Commun.* **245** 37

[19] Leader C 1978 *J. Opt. Soc. Am.* A **68** 175

[20] Xiao X, Ji X L and Lü B D 2008 *Opt. & Laser Tech.* **40** 129

[21] Shirai T, Dogariu A and Wolf E 2003 *J. Opt. Soc. Am.* A **20** 1094

[22] Young C Y, Gilchrest Y V and Macon B R 2002 *Opt. Eng.* **41** 1097